SANDIA REPORT

SAND2014-19199
Unlimited Release
Printed October, 2014

A Handbook on Artificial Soils for Indoor Photovoltaic Soiling Tests

Patrick D. Burton, Bruce H. King

Prepared by
Sandia National Laboratories
Albuquerque, New Mexico 87185 and Livermore, California 94550

Sandia National Laboratories is a multi-program laboratory managed and operated by Sandia Corporation, a wholly owned subsidiary of Lockheed Martin Corporation, for the U.S. Department of Energy's National Nuclear Security Administration under contract DE-AC04-94AL85000.

Sandia National Laboratories

Issued by Sandia National Laboratories, operated for the United States Department of Energy by Sandia Corporation.

Available to DOE and DOE contractors from
U.S. Department of Energy
Office of Scientific and Technical Information
P.O. Box 62
Oak Ridge, TN 37831

Telephone: (865) 576-8401
Facsimile: (865) 576-5728
E-Mail: reports@adonis.osti.gov
Online ordering: http://www.osti.gov/bridge

Available to the public from
U.S. Department of Commerce
National Technical Information Service
5285 Port Royal Rd
Springfield, VA 22161

Telephone: (800) 553-6847
Facsimile: (703) 605-6900
E-Mail: orders@ntis.fedworld.gov
Online ordering: http://www.ntis.gov/help/ordermethods.asp?loc=7-4-0#online

SAND2014-19199
Unlimited Release
Printed October, 2014

A Handbook on Artificial Soils for Indoor Photovoltaic Soiling Tests

Patrick D. Burton & Bruce H. King
Sandia National Laboratories
PO Box 5800
Albuquerque, NM 87185

Abstract

This manuscript is intended to serve as a practical guide to conducting repeatable indoor soiling experiments for PV applications. An outline of techniques, materials and equipment used in prior studies [1–3] is presented. Additional recommendations and practical guidance has been presented. Major sections include techniques to formulate soil simulants, ('standard grime') and feedstocks from traceable components, spray application, and quantitative measurement methodologies at heavy and minimal soil loadings.

Acknowledgment

This work was supported by the U.S. Department of Energy SunShot Initiative.

The authors thank Liza Boyle, Sravanthi Boppana, Vidyashree Rajasekar and Govindasamy Tamizhmani for insights and discussion to improve this project.

Contents

Appendix

Figures

Tables

Nomenclature

PV Photovoltaic

QE Quantum efficiency; a measurement of the number of electrons available to an external circuit per incident photon.

Grime Used specifically to denote artificial soil onto photovoltaic surfaces, chiefly low-iron borofloat glass.

$\overline{M}$ Average mass loading of test coupons determined by triplicate measurements of clean and soiled glass divided by the area determined by image analysis.

PSD Particle size distribution

ACN Acetonitrile, (CH_3CN) a high volatility solvent used as a carrier for suspended grime.

Munsell swatch A color notation system where the hue is followed by value and chroma. For example, 5YR 5/8 indicates a hue of 5YR (a medium yellow-red), value of 5 (medium) and chroma of 8 (high).

mc-Si Multicrystalline Si PV cell

1 Introduction

1.1 Background

Soil accumulation on photovoltaic (PV) modules presents a challenge to long-term performance prediction and lifetime estimates due to the inherent difficulty in quantifying irregular changes over a large area for an extended period. Predictive estimates are usually unavailable until after a system has been deployed and monitored for a year or more. As a result, estimates are used in long-term models [4]. Thevenard and Pelland [4] noted that uncertainty in the performance evaluation of large systems presents a challenge to assessing economic viability. In an example calculation, the authors estimated a 3% derate factor with 2% uncertainty, assuming that rain would be sufficient to clean the panels. They noted that their estimates could be improved with a better understanding of soiling losses. In arid regions, an extreme value for transmission loss due to soiling was reported by Elminir et al. [5]. As dust continued to accumulate, the surface eventually saturated; making the effect of additional particulates insignificant. Beattie et al. [6] has described this effect as a function of particle stacking. In an indoor experiment, sand particles were applied in a narrow size distribution to glass surfaces. The total obscured area of the slide was an exponential function of particle clustering. Mani and Pillai [7] have metaphorically described this clustering effect as "dust promotes dust".

These maximum soiling limits may be met in extreme environments [8], but a more frequently encountered challenge is to determine the point at which modules should be cleaned. A strictly time-based cleaning regime does not adequately account for the variability experienced by each individual system. It is more appropriate to clean systems based on the mass loading of accumulated soil. However; correlating mass loading to performance remains difficult. A discrepancy between models for heavy mass loadings and lighter coatings has been noted in the literature [9]. Alfaro et al. [10] found a non-linear change in haze at low mass loadings (< 1 g/m^2). As the amount of material increased above 1 g/m^2, the change became linear. The authors postulated that in the low soiling limit, soil particulates function as individual scattering points, whereas more dense coatings cause multiple scattering. This effect may be further complicated for assembled PV modules, which have glass, encapsulant, and possibly anti-reflection layers between the soil and PV device.

In addition to system performance prediction, resource-efficient cleaning could benefit greatly from a better understanding of PV soiling. A simple water spray is effective for light dust, but requires a substantial time investment for large systems in addition to the resource consumed [11]. Soil mitigation is therefore best thought of as an opportunity cost for each time interval (daily, weekly, monthly, etc.). Determining a minimum soiling level for flat plate PV can help determine the point where the gain in output (Figure 1, arrow a) exceeds the cleaning expense (Figure 1, arrow b). Certain soil types (illustrated in Figure 1 as line 2) may significantly interfere with light transmission, making almost any cost to remove them worthwhile. Soils with a high soot content obscure light very effectively [1]. Cleaning systems in an urban environment would most likely be a worthwhile undertaking, despite

the difficulty of removing organic and carbonaceous residues. In contrast, other soil types (e.g. line 3) may obscure relatively little light, or be so difficult to remove that the cleaning cost is difficult to recover.

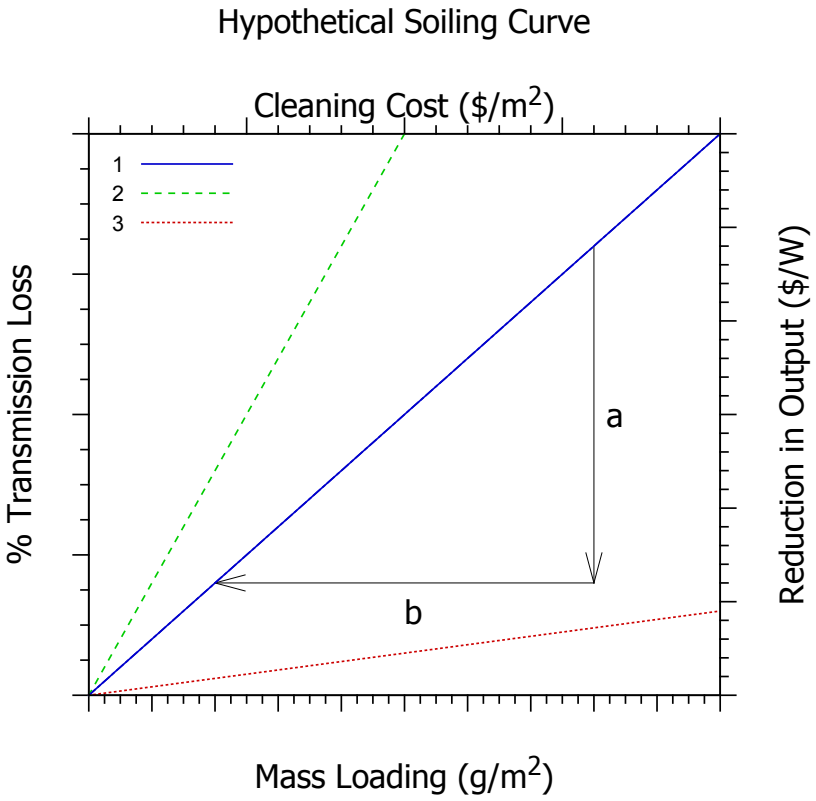

Figure 1. Illustration of hypothetical soiling curves and the benefit (line a) to cost (line b) ratio to clean affected systems.

Precise information regarding soil type and system loss is, naturally, system and location specific. Daily losses during periods without rain have been calculated [12] at 0.2%, which can result in annual losses of 1.5 to 6% in some regions. However; more generalized information for regions and common PV types can be useful for predicting dereates and associated maintenance costs for a planned installation. Specifically, a thorough understanding of the optical interactions between incident light and soil particulates can be used to determine the minimum soil loading associated with appreciable performance loss.

1.2 Artificial Soiling

In order to better understand soiling effects, repeatable measurements are needed. Repeatable soiling conditions can only be achieved using controlled soil composition and deposition

techniques. In this handbook, we describe the formulation of a soil analogue, described as 'standard grime' to differentiate it from natural soil. The grime was formulated from consistent, reproducible feedstocks, as explained in section 2. A repeatable deposition technique is described in section 3. Quantification methods are presented in section 4. A discussion on a minimum soiling limit is presented in section 5.

1.3 Safety

The techniques presented in this manuscript present several potential hazards which must be mitigated. Broadly, this technique is a pressurized application of respirable particles suspended in organic solvents. Suitable air handling must be available to prevent solvent or particle inhalation. Basic personal protective equipment (PPE) includes solvent-resistant gloves (butyl rubber) and eye protection when handling solvents. Solvents should be handled away from any ignition sources; especially when aerosolized by the spray applicator. Operators should be familiar with the safety data sheet (SDS) of any chemical used. Users should likewise be familiar with the operation of any pressure system used. More specific safety information is discussed in detail in subsection 3.3.

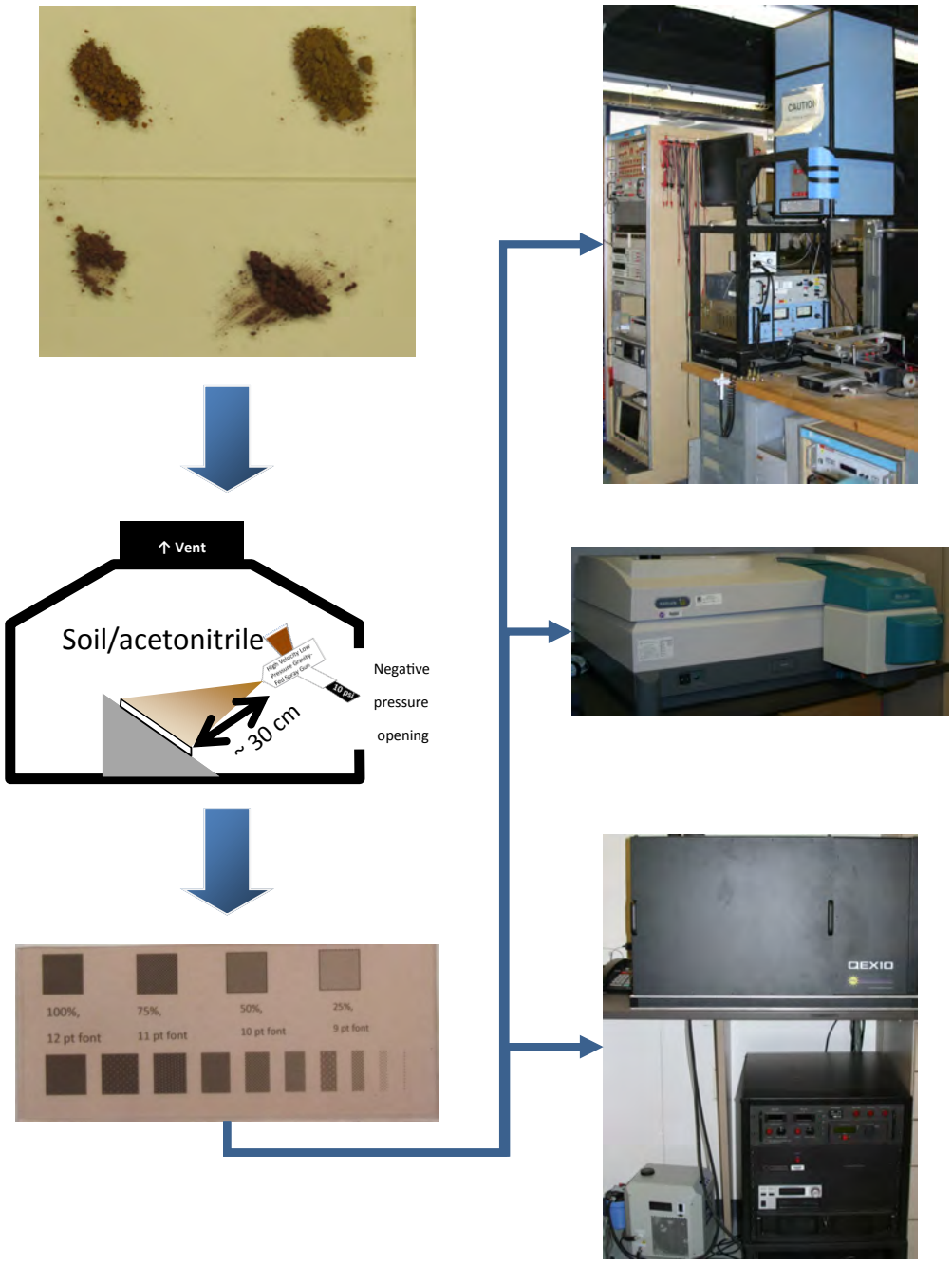

Figure 2. Schematic of the techniques described in this handbook. Soil analogues are formulated using controlled components, applied to test coupons in a repeatable manner and analyzed using complimentary instrumentation.

2 Standard Grime Formulation

This section will summarize the grime formulation procedures used to prepare reproducible soil simulants. Where possible, components were obtained from commercial (and preferably traceable) sources. However, many natural soil components are not available as commercial products, so repeatable synthesis techniques were used to produce consistent test materials.

2.1 Background

A soil analogue was developed by Einfeld et al. [13] to study sample collection efficiency and reproducibility from typical soiled surfaces in an urban environment (New York, NY). Accumulated mineral dust, oils, soot and pollen were of interest to replicate the topical constituents of common surfaces. In order to ensure that a consistent swab collection technique was followed consistently, a soil analogue with a uniform composition was developed and applied to test coupons. This technique has numerous applications to repeatable measurements on PV systems, including optical losses and mechanical wear.

2.2 Formulation Methods for Standard Grime

Base Grime Formulation

In order ensure consistency among samples prepared with a synthetic soil analogue, certified or NIST-tracable components were used whenever possible. Common environmental components, chiefly sand and soot, were replicated using AZ road dust and a soot blend. The components of the soot mixture (Table 1) were dispersed in acetonitrile (ACN) and agitated thoroughly before drying at room temperature. Once dry, the soot was mixed with AZ road dust and ball milled for 48-72 hours. Typically, 97 wt.% AZ road dust was mixed with 3 wt.% soot to produce a blend representative of common urban locations. This differs from the initial composition used by Einfeld et al. [13], as it does not incorporate pollen or spores, which are regulated plant pathogens. In order to accurately replicate soil from a specific location, biological material should be included. However; simulant composition accuracy must be balanced with operational efficiency.

Pigmented Grime Formulation

Modifications to the base grime were made to incorporate spectrally responsive minerals to emulate natural soils. Hematite, a common red mineral, was commercially available as Fe_2O_3 (99.98% trace metals basis, Sigma Aldrich) and used as received. Göthite was not available as a certified or commercial product. Therefore, the material was produced in-house following the method described by Schwertmann and Cornell [14]. While several synthetic

Table 1. Composition of in-house formulated grime blend. The in-house soot composition is expanded upon in the lower row.

Component	Grade	Percent	Source
AZ road dust	A1 Ultrafine, ISO 12103-1	97 wt.%	Powder Technology Inc.
Soot blend	listed below	3 wt.%	see below
black carbon	Vulcan XC-723	83.3 wt.%	Cabot
diesel particulate		8.3 wt.%	NIST catalog # 2975
10W30 motor oil		4.2 wt.%	Home Depot
α-pinene	AC13127-2500	4.2 wt.%	Acros Organics

procedures using acidic or alkaline routes were available, this method was selected as the most broadly applicable. The authors note that the resulting material had "low crystallinity ... [which] resemble goethites from various natural environments" [14]. To produce $\sim$ 6 g of göthite, 0.05 mol (9.9405 g) $FeCl_2{\cdot}4H_2O$ (Fisher, Certified) was dissolved in 1 L of DI H_2O which had been degassed by bubbling N_2 for 30 min. The solution was buffered with 110 mL of 1 M $NaHCO_3$ (Fisher, enzyme grade) and allowed to stir for up to 48 h. The resulting product was filtered and rinsed in DI H_2O and allowed to dry over night prior to analysis. Schwertmann and Cornell [14] provided an alternate synthesis route using $FeSO_4$; however, the resulting material was darker than desired. The $FeCl_2$ route was selected as the preferred route, as it produced soil which matched Munsell swatch 10YR 5.5/8. The Munsell color chart is frequently used in the soil taxonomy community to compare soil color [15, 16]. The chart describes hue, value and chroma for human color perception [17], of which the 2.5 R to 10 YR hue range is commonly used by the USDA for soil color identification [15, 17]. In Figure 3, the hue (color) is arranged about the θ coordinate, while value (lightness) increases in the z direction and chroma (intensity) increases radially. In the highlighted example, color swatch 5YR 5/8 is a medium yellow-red hue, with a medium (5) value and high (8) chroma.

Blends of mineral pigments were used to determine the spectral effects of naturally occurring soils. The desired composition of mineral pigment was mixed with AZ road dust and a small amount of standard grime to yield a mixture that was 40 wt.% pigment, $\sim$59 wt.% dust and $\sim$1 wt.% soot. This mixture had two practical advantages in that reproduction based on composition was easier than formulating a blend to exactly match a particular color swatch, and the primary optical component was the mineral, rather than soot.

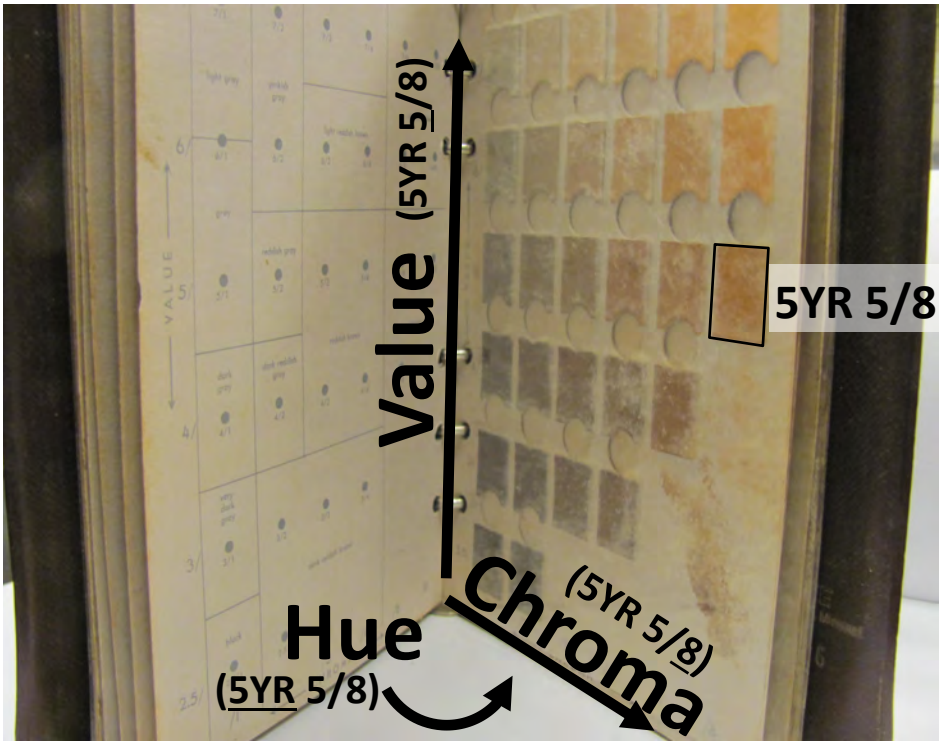

Figure 3. The Munsell color system numerically arranges color swatches on cylindrical coordinates.

Table 2. Composition of mineral pigment grime blends.

Blend	Fe_2O_3	Göthite	Color
40:0	40 wt. %	0 wt. %	10R 3.5/3
30:10	30 wt. %	10 wt.%	2.5YR 3.5/4
10:30	10 wt. %	30 wt. %	7.5YR 5/4
0:40	0 wt. %	40 wt. %	10YR 4/4

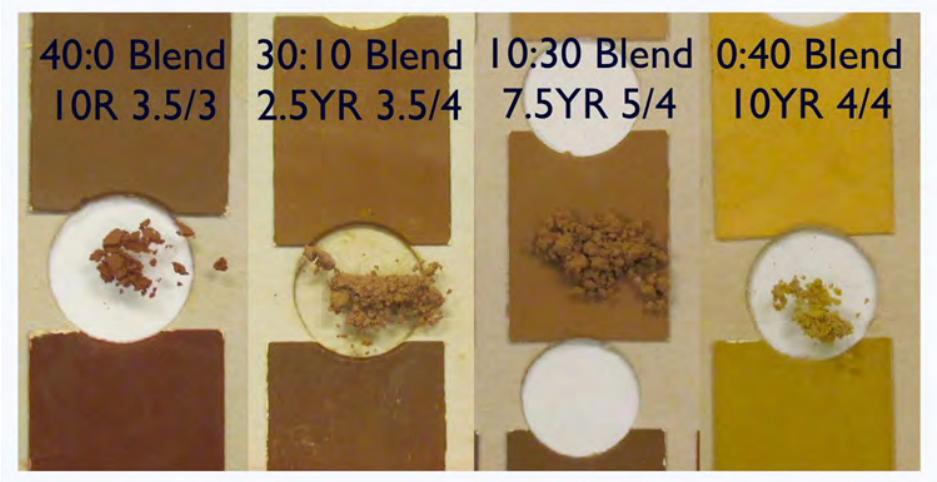

Figure 4. Images of the pigmented grime powders. Note that the image is not calibrated for color and is provided as a rough illustration only.

3 Grime Application

This section will present an overview of the grime deposition technique. Specific information regarding lessons learned and optimal usage will be provided, with the intent that this method could be replicated by other laboratories to establish a location and time-independent method to evaluate soiling losses on PV systems.

3.1 Suspension in ACN

The prepared grime powder was dispersed in ACN as a carrier solvent to ensure fast drying. This deposition technique was intended to emulate gradual aerosol deposition. Grime was suspended in ACN at a ratio of 12 g/l of solvent. Subsequent work [3] demonstrated that variations in suspension concentration could be used to vary the deposition pattern. Each grime blend was prepared at the time of use by adding the desired amount of dry grime powder to an appropriate volume of solvent. Typically, the batches were prepared to ensure that the entire batch would be consumed by the preparation of a single set of coupons. The suspension was gently agitated by shaking the sealed container, and transferring the liquid to the spray gun hopper. If any suspension was left, it would be used within a few days by shaking gently to re-suspend. Sonication was not needed, and intentionally avoided to limit any damage to the mineral particulates.

3.2 Substrate Selection and Surface

For best results, a low iron glass should be used to reduce noise in the transmission measurements. Schott Borofloat 33 was selected since it is described by the manufacturer [18] as a PV material. When float glass is produced, the side in contact with molten tin will be slightly rougher than the opposite side once cool. In order to maintain sample consistency, the non-tinned side of each coupon was used as the grime deposition surface. The tinned side can be determined by touch. After cleaning the sample, a tissue placed over a gloved finger provides sufficient tactile feedback to distinguish the rough side. See section 4 for further discussion on glass selection, and subsection 4.1 for detail on gravimetric analysis. If the glass coupons are cut to a specific size, caution should be exercised to avoid cuts from the glass edge or any generated debris.

The surface that the grime is deposited on is significant to later results. To illustrate, data from a field-collected sample has been included below. This sample was installed in an outdoor collection frame with the rough face of the glass exposed for sample collection. Initial reflectance data for this sample did not follow the expected trend. On further examination, it was determined that the soil was deposited on the rough face, while the clean reference coupon was scanned with the smooth face facing the detector. As a result, the calculated difference between sample and baseline was outside the expected range. A replicate test was conducted with the reference coupon oriented with the rough face to the detector, and

the resulting scan correlated to the samples, as shown in Figure 5a. A similar test of the transmission data could not distinguish the rough side of the blank coupon from the smooth side (Figure 5b). In order to ensure the greatest repeatability between sample sets, it is recommended to ensure that soil is always deposited on the smooth side of the glass.

3.3 Specific Safety Concerns

The application process includes toxic, flammable solvents and respirable particles, which must be handled safely. The ACN carrier solvent should always be handled in a chemical fume hood or, if unavailable, a ventilated spray chamber. Aerosolizing a flammable solvent is a fire hazard, and should be done away from any source of ignition. The tent shown in Figure 7 is operated under negative pressure to prevent contact with the solvent and aerosolized particulates. An advantage to using a dedicated ventilated tent is that sample cross-contamination can be reduced or eliminated. The tent should be HEPA-filtered and connected to an adequate chemical fume exhaust. The spray applicator is a low pressure device, which reduces, but does not eliminate, the hazards associated with a pressurized system. Caution should be exercised when operating the sprayer within the spray chamber or fume hood. Protective eyeware and solvent-compatible gloves should be used when handling solvents, pressure systems, or (if used) glass cutting tools.

When assembling the sprayer (Figure 6), each part should be inspected for damage prior to use. The assembled gun should be lubricated with a small amount of neat solvent before applying grime. After use, flush the hopper with neat solvent before disconnecting from the pressurized gas line. Dismantle the unit inside the ventilated chamber in case any residual solvent remains. The fluid contact parts (nozzle and pin) should be sonicated to remove any residual grime.

3.4 Application Technique

A commercial high velocity low pressure (30 psi) detailing gun was used to disperse the grime and allow the aerosolized suspension to settle on the glass surface. The high volatility of the ACN carrier solvent ensured that the droplets would dry quickly once settled on the glass surface. Aerosolization was conducted in a HEPA filtered tent with negative pressure to mitigate exposure hazards due to the ACN and dispersed particulate matter. Since the spray plume was aimed in the direction of air flow, there was no significant effect of air currents on the aerosol deposition. Sample coupons were placed on an elevated platform approximately 30 cm from the tent opening and tilted at a 45° angle. This placement ensured that the sprayer could be consistently held at the same position. Heavy mass loadings were achieved by repeating the spray process multiple times, as needed. Generally, coatings were applied until the grime suspension was fully consumed, and the resulting mass loading was determined after the final coat. If a specific mass loading was desired, the coupon would be weighed between coating steps to ascertain the mass. This practice is not recommended; as

Table 3. Parts list and sample arrangement for HVLP sprayer and coupons, shown in Figure 6.

Piece	Name	Comments
a	sample coupons	Large glass sheets were used to position the sample coupons (microscope slides and longitudinal glass piece) in the approximate center of the stage.
b	spray nozzle	Aerator wings were always positioned horizontally. Effort should be made to align this piece in the same position during reassembly.
c	spray gun body	The flow control (knob near the trigger) was opened a half turn, and the inlet knob near the air intake was fully open.
d	piston	The grime suspension is abrasive and will slowly corrode the contact surfaces. The entire unit should be replaced periodically ($\sim$ 3 months) or sooner if damage is evident.
e	spring	
f	end cap	This model has a thread stop to control the depth which the trigger can be pulled. The thread stop was set to allow a full trigger pull.

handling the coupon frequently while determining the mass can lead to measurement errors.

When spraying a series of coupons [1], or a single long piece [2], the sprayer was held at the upper right corner and aimed passed the leading edge of the sample. Once the trigger was pressed, the sprayer was swept at a steady rate over the entire coupon, until the spray plume reached the opposite edge of the coupon, when the trigger was released. Starting the spray at the leading edge ensured that the entire sample was coated by the plume in motion, reducing edge effects as much as possible. When single, isotropic coupons were coated [3], the plume was centered over the coupon and very brief bursts were applied. In both cases, the application time was minimized and pauses were made between coats to ensure that there was no residual solvent on the surface. As the grime coating density increased, the solvent evaporated more slowly. An evaporation front could be easily observed, and once the coupon was completely dry, the next coat was applied. Some discrepancy was noted between the samples prepared with a sweeping motion and motionless techniques. Very heavy mass loadings were easier to achieve when using a sweeping motion. Sample uniformity was also greater when using the sweeping motion, as shown by the differences in Figure 8a and Figure 8b. The swept and motionless samples have similar mass loadings (0.131 and 0.133 g/m^2, respectively); however, the motionless sample exhibits a slight mottled texture. This texture is likely due to the evaporation of pooled solvent on the glass surface.

In addition to spray technique, the hardware influences the resulting pattern. The grime is abrasive and will damage the sprayer spindle over time. Regular replacement is recommended in order to maintain sample consistency. After spray application, the sprayer should be

dismantled and cleaned by sonicating all removable fluid contact parts (spindle and nozzle head) in deionized water. Once cleaned, dry and reassembled, fresh solvent should be passed through the sprayer to wet and lubricate the fluid contact parts immediately prior to use.

Patterned Grime

Natural soil accumulation is often non-uniform due to weather and sporadic deposition. Fielded modules often exhibit raindrop patterns due to incomplete washing during light rain or dew events. The basic grime application technique was modified to emulate these patterns. By mixing a less volatile solvent (ethanol) with the ACN carrier solvent, a phase separation was induced. The grime aggregated in islands formed by the immiscible solvents, as shown in Figure 9b. While the individual islands on each sample produced with this technique were unique, the overall texture produced was reproducible. The use of highly immiscible solvents, such as ACN and hexane, is not recommended, as the strong polar/non-polar segregation produced very inconsistent coatings.

To produce a grime pattern with non-uniform spot sizes, the concentration of the grime suspension was increased. This produced a grime sputter coat rather than a homogeneous spray.

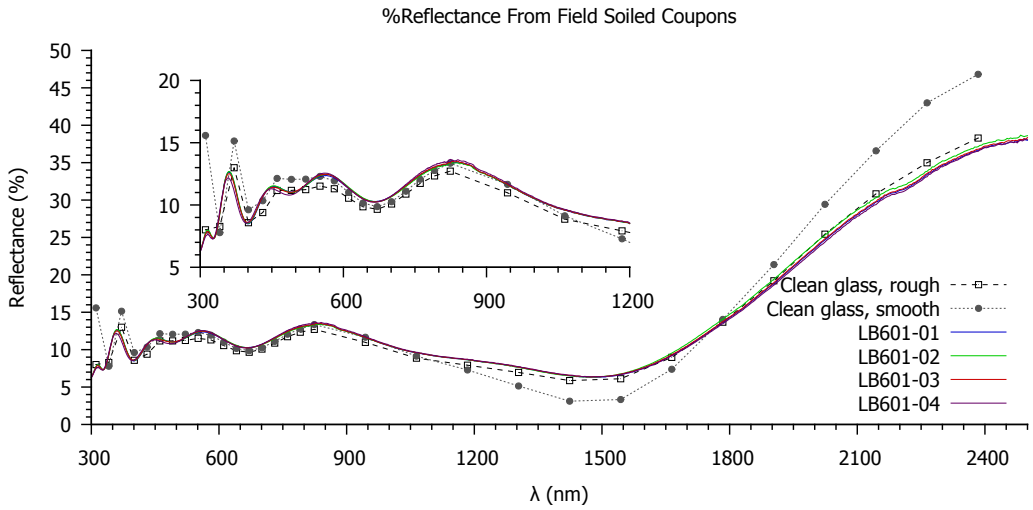

(a) Reflectance

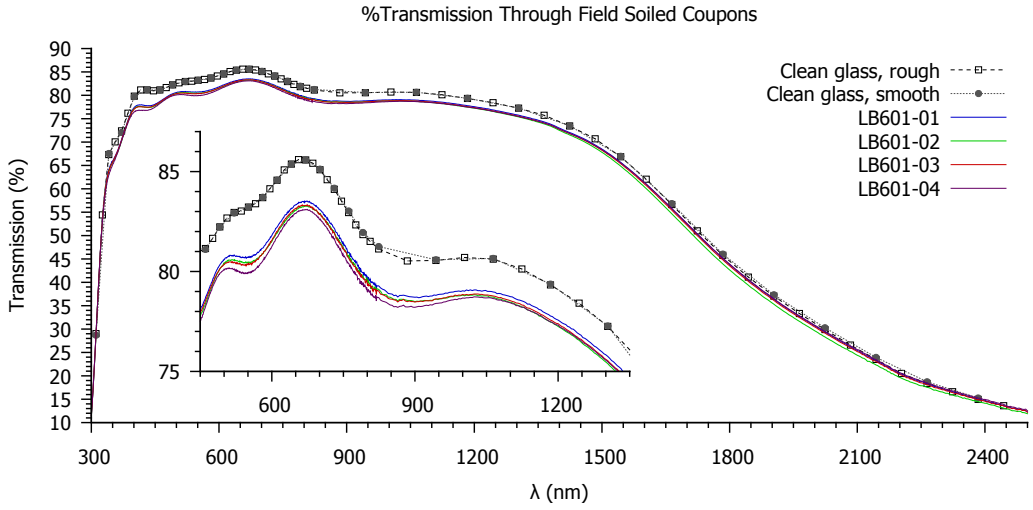

(b) Transmission

Figure 5. Reflectance (a) and transmission (b) plots illustrating the difference between the smooth and rough surfaces of the reference coupon.

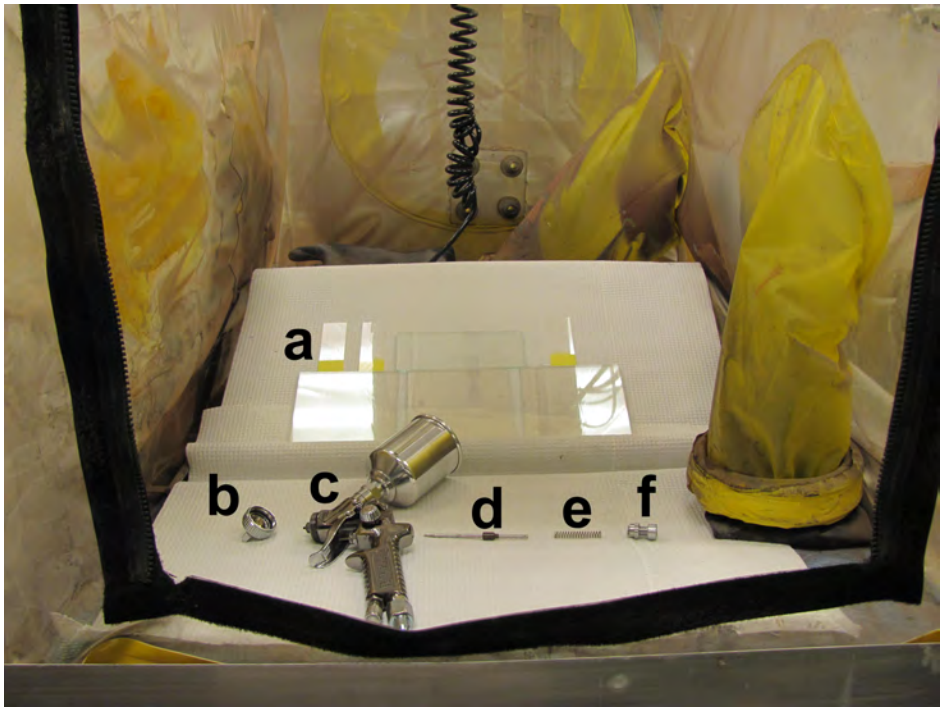

Figure 6. Image of spray equipment inside the HEPA-filtered tent. Identified parts are described in detail in Table 3

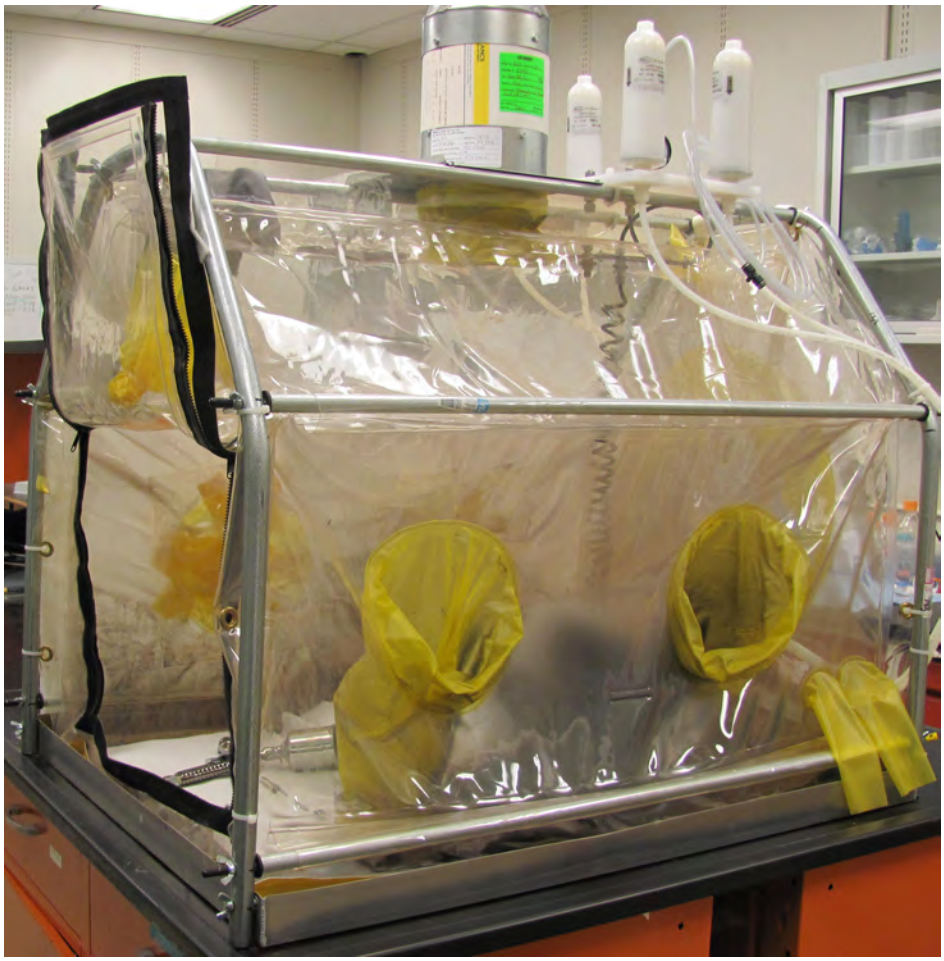

Figure 7. Exterior image of the HEPA-filtered tent, showing duct to local exhaust.

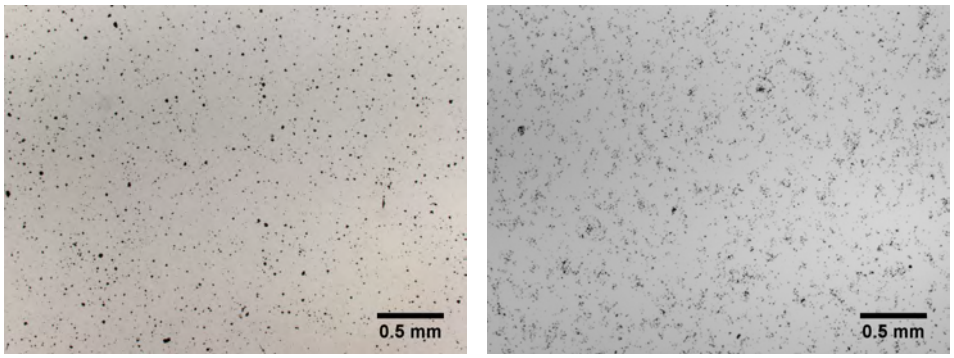

(a) Swept Spray (b) Motionless Spray

Figure 8. Images of grime pattern produced using a swept spray (a, 2.3% area coverage) and motionless spray (b, 4.4% area coverage).

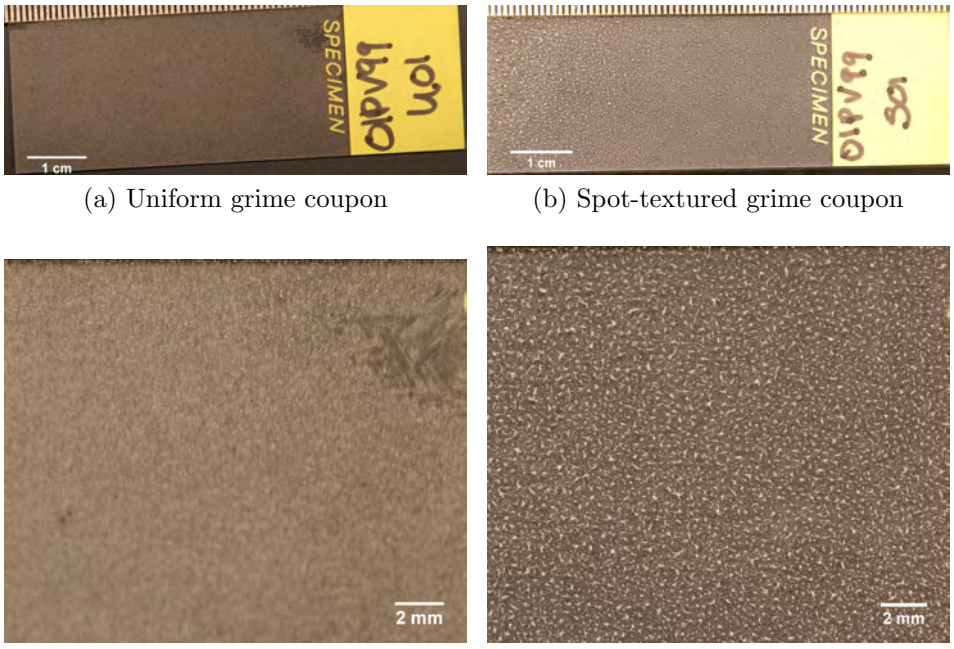

(a) Uniform grime coupon (b) Spot-textured grime coupon

(c) Close-up of uniform grime coupon (d) Close-up of textured grime coupon

Figure 9. Images of soiled coupons with uniform (a, c) and spot-textured (b, d) patterns.

4 Quantitative Laboratory Methods

The optical effects of soil on PV, CPV and CSP systems have been a concern for many years [19]. Replicating the effects of soil in a controlled and repeatable manner presents several challenges. Indoor tests require several simplifications, such as the use of small glass coupons as a surrogate for soiled modules.

An assembled PV module consists of several intermediate layers, such as a transparent conductive oxide, encapsulant, and anti-reflective coatings between the glass and PV cell. Instead of attempting to replicate the optical effects of each of these components in tandem with the applied grime, the optical effect of the grime itself was determined by comparing the light transmission through soiled and reference glass coupons. A small discrepancy is introduced by using an independent reference rather than directly measuring the soiled coupon, then subsequently cleaning and remeasuring it. However; using a single reference coupon allows each sample to be used for multiple tests in different instruments. This allows direct comparison between transmission measurements made on a UV/vis spectrometer, quantum efficiency (QE) test stand and 1-sun simulator.

The glass type also influences optical measurements. PV modules are typically constructed using tempered glass for robust performance in the field. Large sheets of tempered glass cannot be cut to produce sample coupons, and small tempered pieces are difficult to acquire. Likewise, many CPV systems use Fresnel lenses, which would be relevant to a soiling study, but are not suitable for the instrumentation used. Direct transmission through a Fresnel lens would require instrument-specific adjustment for the focal length, which is not feasible in the UV/vis spectrometer. CPV testing remains an interesting challenge, but would require grime application to an entire module.

In order to maintain consistency throughout each test, a single glass type was selected and used as a background for each of the three tests. Since the composition of the glass influences the spectrum of the transmitted light, it is recommended that background samples of clean glass be collected independently of the sample. An ambient scan (device or detector only) should be collected first, followed by a scan of the clean reference material, then each successive sample. This enables a better physical understanding of losses caused by the glass and applied grime, respectively.

4.1 Gravimetric Analysis

In order to determine the mass loading of deposited grime, accurate gravimetric analysis was needed. A Mettler Toledo XP205 analytical balance with 0.01 mg readability and 0.015 mg repeatability was used for all measurements. After cleaning and drying the coupons, a sample mark was etched into the top corner of the smooth face (see subsection 3.2) with a diamond scribe. Etching the sample identification mark prior to weighing ensured that the very small change in mass was included in the measurement. Permanent marker should not be used, as it will be dissolved by the grime carrier solvent and contaminate the sample. Likewise,

gloves should be worn when handling the coupons to prevent contamination. Each coupon was placed on the scale until a stable reading was obtained, then removed and followed by the next piece. This procedure was repeated in triplicate by weighing the entire set, then beginning from the same starting coupon. After three measurements had been collected for each coupon, the average and standard deviation were determined (a sample worksheet is included in Appendix B). The average was taken to be the baseline of the clean coupon. After the grime was applied and allowed to dry (see subsection 3.4), the coupons were re-weighed in the same order. The average value was determined, and then subtracted from the baseline to determine the mass of grime applied. In most cases, the value obtained was accepted without returning the coupon to the application stage to apply additional coats. Returning the sample to the application chamber requires additional handling, which should be avoided unless a very specific grime mass loading is required. The area of each coupon was determined by image analysis, as described in subsection 5.2. Once the mass loading had been determined, it was assumed to be constant across the entire coupon. Some film damage was unavoidable when handling the sample, and especially when placed in various sample stages for optical analysis. Subsequent gravimetric analysis to account for blemishes around the edges was not attempted so long as a sufficient probe area remained pristine for each respective optical test.

4.2 UV/vis Spectroscopy

The UV/vis spectrometer is a versatile piece of equipment which can be used in several different configurations to collect relevant transmission and reflectance data. In the standard configuration, the test beam is split between a sample and reference test piece. This provides simultaneous direct (non-scattered) transmission loss through the test coupon relative to the reference. Secondary scattering is not detected in this configuration, making it a useful analogue to changes in direct normal irradiance (DNI). This technique was used to predict the response of triple junction HCPV devices to various soils [20]. It is useful to fully subtract the effect of the substrate by conducting a baseline scan with a clean coupon in both the reference and test positions. The instrument should be set to collect both 100% and 0% baseline scans using the clean test coupon and an opaque beam stopper, respectively. The reference coupon would then be left in position while the test coupon is substituted with samples. The sample holder may dislodge some of the sample, so care should be taken when cycling coupons through multiple tests. Coupons should be oriented to limit any smudges or smears from overlapping the sample collection window. Direct transmission measurements enable a thorough examination of the optical effects of a specific grime, and in particular how various components can inhibit light transmission. For example, in Figure C.1, red grime shows a very small spectral effect, while yellow soil exhibits a significant peak near 425 nm.

While secondary scattering is typically neglected in high concentrating devices, it is a concern in flat plate systems. Therefore, it is useful to use an integrating sphere to collect diffuse transmission measurements in addition to the direct transmission noted above. The incident light passes through the sample (Figure 10) and in to the integrating sphere, where the diffuse and direct portions are collected. In this arrangement, the light scatters through

the glass, so a clean reference coupon was scanned as a sample prior to each test. Influences from the glass are readily noticed, as the response to the red soil in Figure C.2 is very similar to the clean glass, except for a small feature between 600 and 800 nm. The impact of yellow soil is much more pronounced, as a steady decline in transmission can be seen between 300 and 600 nm.

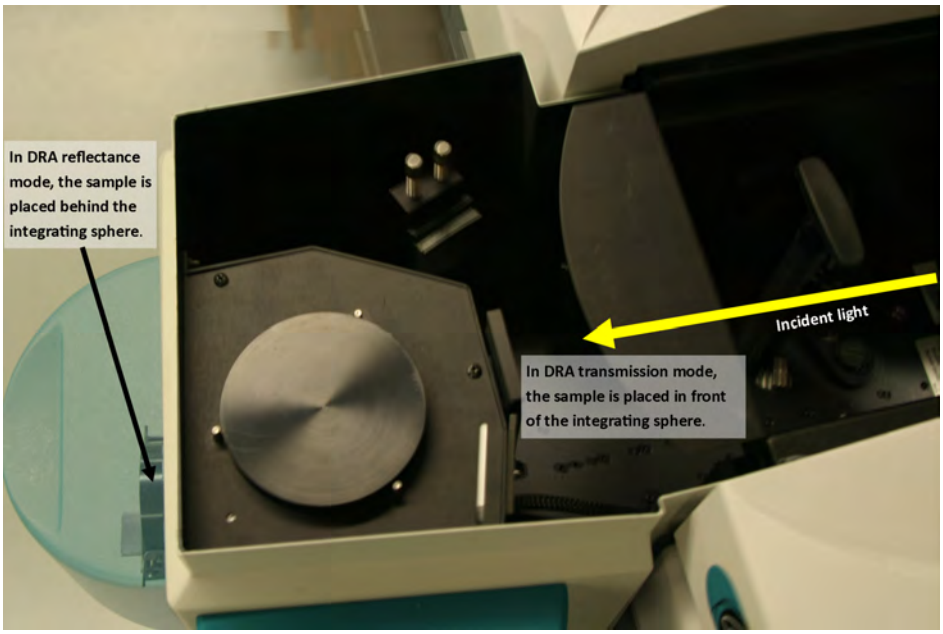

Figure 10. Diagram of the DRA-2500 diffuse reflectance accessory used for transmission and reflectance measurements. In transmission mode, the sample was placed in front of the integrating sphere (right port). Reflectance measurements were collected with the sample behind the integrating sphere, with the grime facing towards the left port. A light trap (shown as a shaded hemisphere) was placed over the test coupon to limit stray light.

An additional capability provided by the diffuse reflectance accessory is a reflectance measurement. The sample coupon is mounted behind the integrating sphere, with the soil facing the beam. Incident light is reflected off of the coupon surface and around the integrating sphere until it reaches the photodiode detector. A basic hemispherical cover was mounted over the external sample clip (Figure 10); however, several secondary reflections are worth mentioning. First, it is important to ensure that the coupon texture is consistent between samples by applying grime to the smoothest (non-tinned) glass face to match refraction indicies between samples. Secondly, the sample port encompasses the majority of the area of a typical glass coupon, and may expose regions that have been scratched during handling. It is advisable to collect reflectance measurements prior to other sample handling that may cause damage to the grime coating. Additionally, care should be taken to prevent grime

from contaminating the reflective surface of the integrating sphere. While reflectance is not immediately correlated to flat plate PV response, it is a useful technique to characterize the optical properties of the grime in conjunction with transmission data. For example, the red soil analogue exhibited a very flat direct transmission profile (Figure C.1), and only minor features in DRA transmission mode (Figure 10). The slight increase observed between 600 and 800 nm in the DRA transmission scan can be seen more clearly in the reflection scan (Figure C.3). The pronounced visible color is entirely due to backscattered light, while the forward scattered light which would reach an underlying PV device (Figure C.1) is comparatively neutral density.

4.3 Quantum Efficiency

Quantum efficiency measurements were collected by placing sample coupons over a test device, in this case, a multicrystalline (mc) Si cell. This method is a somewhat analogous measurement technique to UV/vis transmission, with some significant differences. First, the path length from the surface of the glass sample to the cell[1] is only as thick as the glass, so scattered light can be collected. Very dense grime films may cause extended scattering, as shown in Figure 11. Secondly, since the glass coupons were used in multiple tests, they

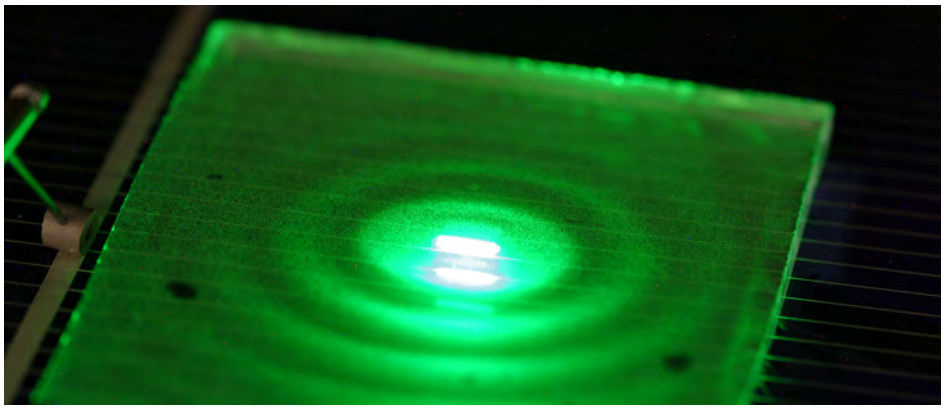

Figure 11. Surface scattering on a densely coated glass coupon. The incident spot should be centered between the crossfingers. Note that the image was collected in a darkened room; scattering is not typically visible under normal illumination.

were not optically coupled to the cell. As a result, the changes in response between the clean reference coupon and soiled samples does not capture the complete behavior of a packaged device. Since the same cell was used for each test, the data collected can be used to understand the trend associated with different soil types and mass loadings (Figure C.4).

[1]The cell is essentially a detector, albeit not as sensitive or calibrated like the diode in the spectrometer.

When preparing for a test, the cell should be aligned to the instrument beam in a consistent position. For multicrystalline cells, the same crystallite can be used as the cell anchor position for each data set, thus improving the repeatability of the test. In the instrument used, it was not feasible to leave the test device in a permanent position, so it is advisable to use a cell with easily recognizable features to guide sample placement. A reference scan of a clean coupon should be collected prior to each session. Comparisons between samples should be made in reference to the clean coupon. Any time the detector or stage is moved, a new reference scan should be collected. Furthermore, the beam size should be adjusted to avoid any edge effects from the bus bars or crossfingers. If the beam overlaps features on the device, an incorrect reading will result.

4.4 One Sun Simulator

The one-sun simulator provides the most immediately analogous performance data to outdoor soiling studies. In all of the laboratory studies conducted in this work, a single cell was used as the test device. As discussed in Section 4.3, the device was not optically coupled to the test coupon. The entire exposed active area of the test cell was illuminated, so a separate mc-Si cell[2] was cut to fit. The edges were trimmed at the bus bars, ensuring that the glass coupon would be able to overlap as much of the available area as possible (Figure 12a).

The glass coupons were cut to fit within the 5 cm $\times$ 13 cm sample area between the bus bars. In order to avoid damaging the collection pins, a small overlap was allowed (Figure 12b). This loose gap also improved ease of use, as the coupon could be handled by the edges when needed. Data was always collected using the whole coupon prior to any other tests (UV/vis and QE), where the coupon was subdivided into three portions. Multiple sweeps were collected and averaged to account for any instability in the light source. The average for each set is shown as a point in Figure C.5, with standard deviation in both the current and voltage shown as a shaded area.

[2]Not the same cell used for QE data.

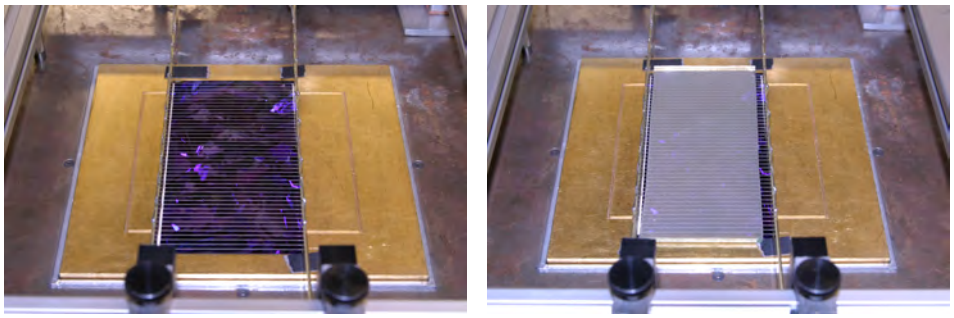

(a) Trimmed mc-Si cell (b) Soiled coupon over cell

Figure 12. (a) Trimmed mc-Si cell placed on one-sun simulator stage. (b) Soiled glass coupon overlapping mc-Si cell, allowing a small gap to avoid damaging the contact pins.

5 Minimum Detection Limit

As photovoltaic devices become increasingly efficient, a greater interest has been placed on balance of systems optimization. For example, recent work [21] has shown a 0.2% change in the overall cell efficiency due to the color of the cell connectors. These incremental improvements in device efficiency could easily be offset by soil accumulation on a fielded device. An effective understanding of the effects of soil accumulation requires a reasonable upper and lower boundary. An upper limit can be readily defined by individual system operators; however, the challenge is to determine a lower bound to soil accumulation. Soil accumulation is a continuous process, so it is necessary to determine a minimum point at which active mitigation techniques are cost effective. For example, El-Nashar [11] has shown that a weekly cleaning regimen for solar thermal desalination collectors in Abu Dhabi yielded optimal production. Cost effectiveness is dependent upon the required frequency as well as the cleaning technique used.

In addition to the soil composition [1], the soil accumulation density is a significant factor to light transmission. For a particular mass loading, a homogeneously distributed soil layer would interact with light in a different manner than the same mass distributed in discrete aggregates. In order to simulate variations in sample deposition, synthetic grime was applied at 10 and 20 g/l concentrations in ACN.

5.1 Sample Coupon Preparation

An absolute minimum to the detectable grime was set by the precision of the scale used to weigh each coupon. Coupons were weighed in triplicate and averaged. The area of each glass coupon was determined by imaging the sample with a ruler included in the field of view (Figure 13a). Each image was imported into ImageJ [22] and calibrated using the known length of the ruler in the image. Auto-level and auto-contrast adjustments were used to enhance the edges of the sample. The glass was outlined by hand since the contrast was not sufficient for automated processing, as shown in Figure 13b. As a result, the area within the boundary was the least reproducible measurement. Each image was re-opened, calibrated, and measured in triplicate to generate a sample average and standard deviation.

5.2 Image Processing

Applied grime patterns were analyzed using ImageJ [22]. Automated image analysis does introduce some error, which is important to consider. Since the particulate sizes were widely distributed, a single magnification setting was insufficient to capture the entire dimensional range.

Background subtraction was attempted with some images. The rolling ball radius was set to 5.0 pixels with a light background option. This produced a washed-out image as

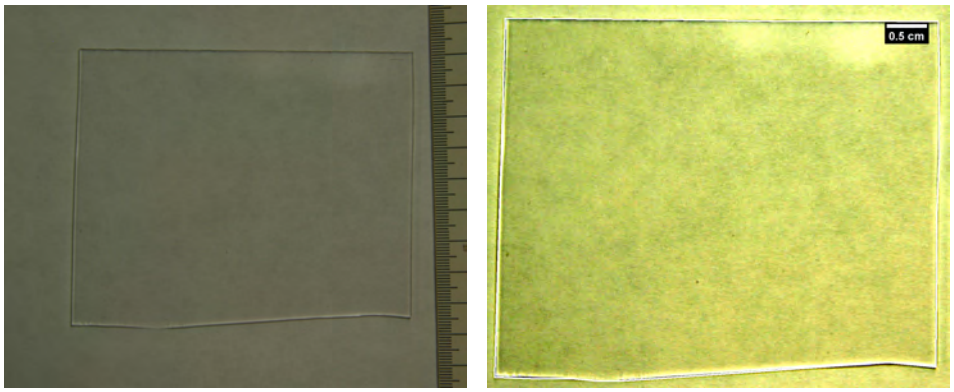

(a) Raw image of soiled coupon (b) Processed image showing outline

Figure 13. Images of soiled coupons were collected (a) and analyzed in ImageJ (b) to find the total area of the glass.

seen in Figure 14b. The contrast was enhanced to 0.4% saturated pixels, and an automatic threshold was applied to generate the binary map shown in Figure 14c.

(a) Original (b) Background removed (c) Binary image map

Figure 14. Image processing in ImageJ to find the particle size distribution.

Automated background subtraction was not suitable for all images, so in order to maintain consistency, a simplified counting technique was used. Code for an ImageJ macro is included in Appendix A

5.3 Measurements

Instrumental measurements were substantially more repeatable than determining the grime mass loading, in most cases. Triplicate measurements were collected for the QE and UV/vis measurements to generate the error bars shown in Figure 15. Shaded regions indicate data points for which the standard deviation σ_{mass} of the mass loading is greater than 25% of the magnitude of the measurement.

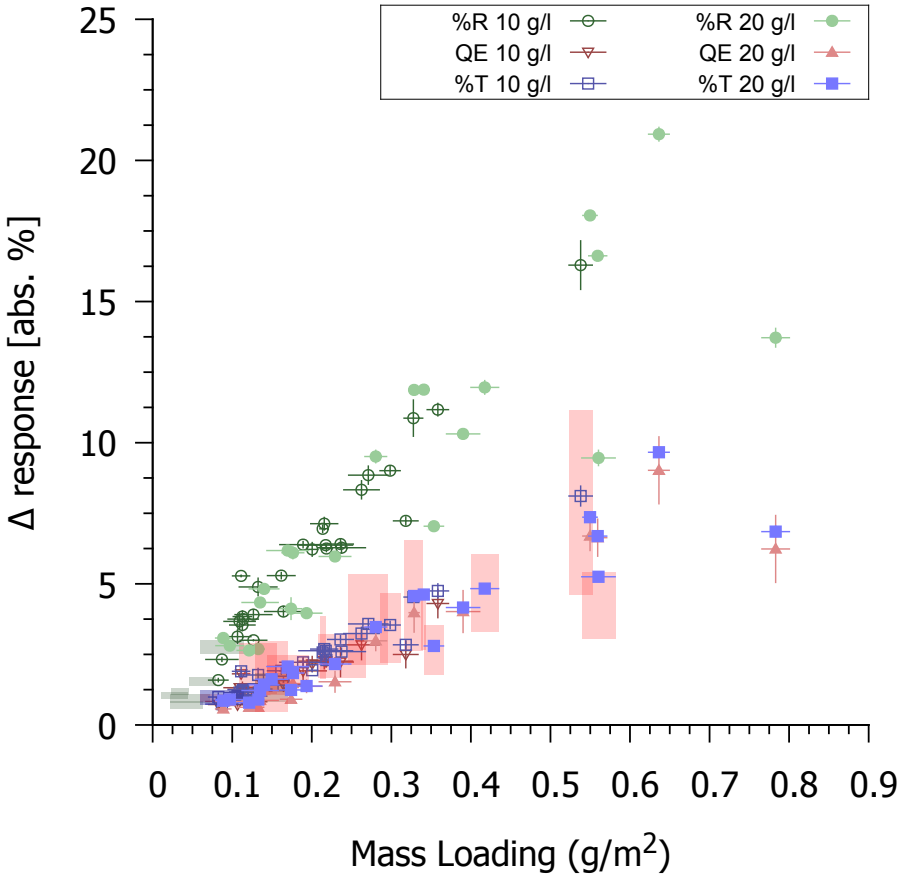

Figure 15. Change in measured response for low mass loadings. Error bars indicate width of the standard deviation of 3 repeat measurements. Any σ greater than 25% of the total magnitude (in either the x or y direction) is shown as a shaded bar rather than a point and line. This figure will be referred to frequently throughout this section.

One-Sun Simulator

One-sun simulator measurements were collected; but due to the poor data quality, could not be relied upon to show any meaningful trend. This is most likely due to the inexact size match of the reference coupon and test coupons. Since the one-sun simulator is a broad beam[3] test, the entire coupon is illuminated at once. As a result, deviations in the sample area are incorporated into the test. This area could not be easily normalized across each sample. Additionally, instrumental fluctuations in the simulator made the measurements unreliable. The average ΔJ_{SC} of most samples was less than zero, suggesting that coupon area mismatch (see discussion in Section 4.4) was a more significant factor than surface contaminants.

Reflectance

In contrast, reflectance measurements provided a much better signal to noise ratio, enabling easy discrimination between clean coupons and the lightest grime coatings. Note that each of the traces shown in Figure 16 is a composite of three overlapped scans. The individual traces can be seen more clearly in the inset. The data set marked by a star (*) was below the mass detectability limit, and corresponds to the lowest shaded point in Figure 15 (green square). Even though the mass could not be adequately measured, the reflectance data for this point is easily distinguished from the clean glass reference. Reflectance measurements were speculated to be the simplest field monitoring method due to the significantly greater response. While reflectance does not correlate directly to PV performance, it can be used as a proxy to determine soil accumulation. The magnitude of the response is much greater, but the overall trend between reflectance and transmission measurements is similar at low ($> 0.4\ g/m^2$) mass loadings. Above this limit, reflectance increases rapidly. This rapid increase is not useful for quantitative measurements, but is very applicable to qualitative field measurements. Any reflectance change above a certain threshold could be used as a benchmark for cleaning (especially large) systems. This could substantially improve the operational cost of systems in regions with moderate expected soil losses.

Work by Murphy and Forman [23] used a glossmeter to determine soil loading on fielded modules, reporting only in terms of measured gloss. These measurements were not directly correlated to mass loading; however, the authors reported a particle composition effect in later work [24]. The authors emphasized composition rather than particle size as the primary property of interest. Reflectance measurements do provide good repeatability (Figure 15), but do not directly correlate to the physical behavior of light impinging on a PV device. A simple change in reflectance does not simultaneously account for both particle size and mass density on the substrate.

[3] and broad spectrum

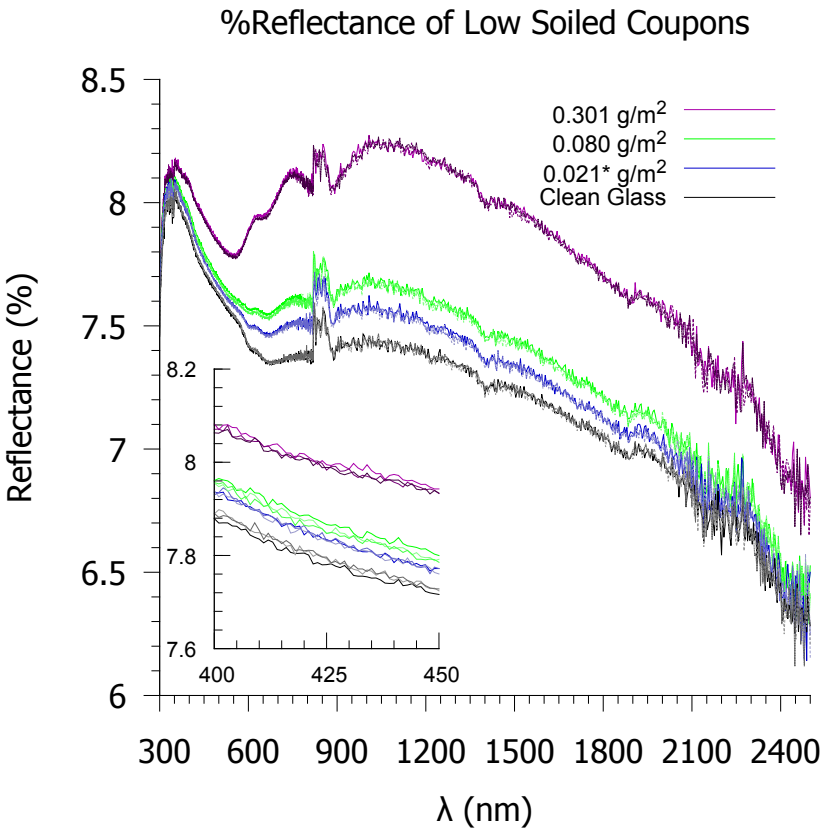

Figure 16. Reflectance measurements provided the most distinct delineation between each sample. Each data set shows triplicate measurements (higher resolution inset).

Quantum Efficiency

As discussed previously, grime texture influences light transmission. This effect is particularly pronounced for the QE instrument. The sample is in close proximity to the detector (a multicrystalline Si cell), on which the incident light beam is focused to a small spot. As a result, grime aggregates on the surface are very large relative to the beam spot. Non-uniform particle distribution causes significant shadowing, making repeat measurements difficult. Scans were collected in various regions across the soiled glass coupons, near the top, middle and bottom of the approximate center of each coupon. These measurements were much more sensitive to sample homogeneity, and many results were outside the acceptable range of $\sigma > 25\%$ of the magnitude (Note the numerous red shaded squares in Figure 15).

References

[1] P. D. Burton and B. H. King. Application and Characterization of an Artificial Grime for Photovoltaic Soiling Studies. *Photovoltaics, IEEE Journal of*, 4(1):299–303, 2014. doi:10.1109/jphotov.2013.2270343.

[2] P. D. Burton and B. H. King. Spectral Sensitivity of Simulated Photovoltaic Module Soiling for a Variety of Synthesized Soil Types. *Photovoltaics, IEEE Journal of*, 4(3): 890–898, 2014. doi:10.1109/JPHOTOV.2014.2301895.

[3] P. D. Burton and B. H. King. Determination of a Minimum Soiling Level to Affect Photovoltaic Devices. In *IEEE 40th Photovoltaic Specialists Conference*, pages 0193–0197, 2014. doi:10.1109/pvsc.2014.6925529.

[4] D. Thevenard and S. Pelland. Estimating the uncertainty in long-term photovoltaic yield predictions. *Solar Energy*, 91(0):432–445, 2013. doi:10.1016/j.solener.2011.05.006.

[5] H. K. Elminir, A. E. Ghitas, R. H. Hamid, F. El-Hussainy, M. M. Beheary, and K. M. Abdel-Moneim. Effect of dust on the Transparent Cover of Solar Collectors. *Energy Conversion and Management*, 47(18-19):3192–3203, 2006. doi:10.1016/j.enconman.2006.02.014.

[6] N. S. Beattie, R. S. Moir, C. Chacko, G. Buffoni, S. H. Roberts, and N. M. Pearsall. Understanding the Effects of Sand and Dust Accumulation on Photovoltaic Modules. *Renewable Energy*, 48(0):448–452, 2012. doi:10.1016/j.renene.2012.06.007.

[7] M. Mani and R. Pillai. Impact of Dust on Solar Photovoltaic (PV) Performance: Research Status, Challenges and Recommendations. *Renewable and Sustainable Energy Reviews*, 14(9):3124–3131, 2010. doi:10.1016/j.rser.2010.07.065.

[8] C. Schill, S. Brachmann, M. Heck, K.-A. Weiß, and M. Köhl. Impact of heavy soiling on the power output of PV modules. In *Proc. SPIE*, volume 8112, page 811207, 2011. doi:10.1117/12.893721.

[9] L. Boyle, H. Flinchpaugh, and M. Hannigan. Impact of Natural Soiling on the Transmission of PV Cover Plates. In *IEEE 39th Photovoltaic Specialists Conference*, pages 3276–3278, 2013. doi:10.1109/PVSC.2013.6745150.

[10] S. C. Alfaro, A. Chabas, T. Lombardo, A. Verney-Carron, and P. Ausset. Predicting the soiling of modern glass in urban environments: A new physically-based model. *Atmospheric Environment*, 60(0):348–357, 2012. doi:10.1016/j.atmosenv.2012.06.050.

[11] A. M. El-Nashar. Seasonal effect of dust deposition on a field of evacuated tube collectors on the performance of a solar desalination plant. *Desalination*, 239(1-3):66–81, 2009. doi:10.1016/j.desal.2008.03.007.

[12] A. Kimber, L. Mitchell, S. Nogradi, and H. Wenger. The Effect of Soiling on Large Grid-Connected Photovoltaic Systems in California and the Southwest Region of the United

States. In *IEEE 4th World Conference on Photovoltaic Energy Conversion*, volume 2, pages 2391–2395, 2006. doi:10.1109/wcpec.2006.279690.

[13] W. Einfeld, R. M. Boucher, M. S. Tezak, M. C. Wilson, and G. S. Brown. Evaluation of surface sampling method performance for *Bacillus* Spores on clean and dirty outdoor surfaces. Technical Report SAND2011-4085, Sandia National Laboratories, 2011.

[14] U. Schwertmann and R. M. Cornell. *Iron Oxides in the Laboratory Preparation and Characterization*. Wiley-VCH, Hoboken, NJ, Second, Completely Revised and Extended edition, 2000.

[15] Soil Survey Staff. Soil Taxonomy: A Basic System of Soil Classification for Making and Interpreting Soil Surveys. Technical Report 436, 1999. Natural Resources Conservation Service. U.S. Department of Agriculture.

[16] J. Torrent and V. Barrón. The visible diffuse reflectance spectrum in relation to the color and crystal properties of hematite. *Clays and Clay Minerals*, 51(3):309–317, 2003.

[17] About munsell color. http://munsell.com/about-munsell-color/. Accessed 09/04/2014.

[18] Schott Borofloat® 33 Borosilicate Glass. Online. URL `http://www.us.schott.com/borofloat/english/`. Accessed 07/11/2014.

[19] T. Sarver, A. Al-Qaraghuli, and L. L. Kazmerski. A comprehensive review of the impact of dust on the use of solar energy: History, investigations, results, literature, and mitigation approaches. *Renewable and Sustainable Energy Reviews*, 22(0):698–733, 2013. doi:10.1016/j.rser.2012.12.065.

[20] P. D. Burton, B. H. King, and D. Riley. Predicting the Spectral Effects of Soils on Concentrating Photovoltaic Systems. Submitted to *Solar Energy*.

[21] L. Hamann, L. Prönneke, and J. H. Werner. Colored ribbons achieve $+0.28\%_{abs}$ efficiency gain. *Photovoltaics, IEEE Journal of*, 2(4):494–498, 2012. doi:10.1109/jphotov.2012.2206571.

[22] W. S. Rasband. ImageJ, 1997-2012. URL `http://imagej.nih.gov/ij/`.

[23] E. B. Murphy and S. E. Forman. Measuring Dirt on Photovoltaic Modules. Technical Report COO-4094-37, MIT Lincoln Laboratory, 1979.

[24] E. B. Murphy. Measuring Dirt on Photovoltaic Modules. Part II. Technical Report COO-4094-86, MIT Lincoln Laboratory, 1980.

A Image Processing Macro

This ImageJ macro has been developed to measure particles on a light background following the procedure in Section 5.2. Note that this technique can under-count some of the larger particulates.

```
//Script to process images at 2.52x using background subtraction
 macro "Image Processing (2.52x) " {
    background = File.openDialog("Select the file:");
    open(background);
    run("Set Scale...", "distance=1024 known=2.6 pixel=1 unit=mm");
    setAutoThreshold("Default");
    getThreshold(lower, upper);
    setThreshold(lower, upper);
    run("Convert to Mask");
    run("Analyze Particles...", "size=
       0-Infinity circularity=0.00-1.00 show=Nothing display clear include summarize");
    close();
    selectWindow("Results");
    saveAs("text")
}
```

B Mass Loading Worksheet

Table B.1. Worksheet for grime mass determination.

Sample	Clean	Average	σ	Coated	Average	σ	Grime	σ
Sample 1	Clean 1a Clean 1b Clean 1c	$\overline{\text{Clean 1}}$	σ_{Cln1}	Coated 1a Coated 1b Coated 1c	$\overline{\text{Coated 1}}$	σ_{Co1}	$\overline{\text{Grime 1}}$	σ_{G1}
Sample 2	Clean 2a Clean 2b Clean 2c	$\overline{\text{Clean 2}}$	σ_{Cln2}	Coated 2a Coated 2b Coated 2c	$\overline{\text{Coated 2}}$	σ_{Co2}	$\overline{\text{Coated 2}} - \overline{\text{Clean 2}}$	σ_{G2}

Each clean glass coupon is weighed in triplicate (subsection 4.1) and averaged ($\overline{\text{Clean 1}}$). The standard deviation (σ_{Cln1}) of the average was calculated assuming a normal distribution. This process was repeated for the coated and dried samples to determine $\overline{\text{Coated 1}}$ and σ_{Co1}. The mass of grime applied was calculated as the difference between coated and clean coupons, and the uncertainty propagated as shown in Equation 1.

$$\sigma_{G1} = \sqrt{\sigma_{Cln1}^2 + \sigma_{Co1}^2} \tag{1}$$

Table B.2. Worksheet for mass loading determination by coupon area and measured mass.

Sample	Grime	σ	Area	Average	σ	Mass Loading	σ
Sample 1	$\overline{\text{Grime 1}}$	σ_{G1}	Area 1a Area 1b Area 1c	$\overline{\text{Area 1}}$	σ_{A1}	$\overline{\text{Loading 1}}$	σ_{ML1}
Sample 2	$\overline{\text{Grime 2}}$	σ_{G2}	Area 2a Area 2b Area 2c	$\overline{\text{Area 2}}$	σ_{A2}	$\overline{\text{Grime 2}}/\overline{\text{Area 2}}$	σ_{ML2}

In order to obtain similar statistics for image analysis, each area was determined three times, and used to find an average value and standard deviation. The mass loading was defined as the average mass of grime divided by the average measured area of the coupon. An error estimate was determined by propagating the uncertainty through the entire calculation, as shown in Equation 2.

$$\sigma_{ML1} = \text{Loading 1} \times \sqrt{\left(\frac{\sigma_{G1}}{\text{Grime 1}}\right)^2 + \left(\frac{\sigma_{A1}}{\text{Area 1}}\right)^2} \tag{2}$$

C Example Data

Typical data collected using each of the instruments in subsection 4.4 is shown below.

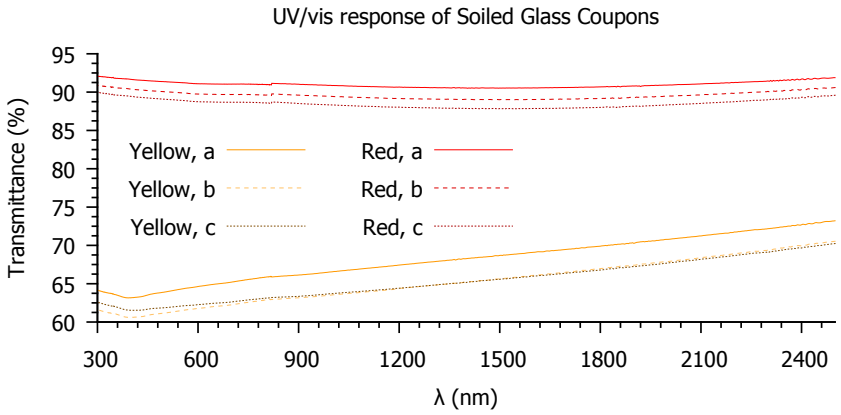

Figure C.1. Direct transmission measured through three coupons each of red and yellow test grime.

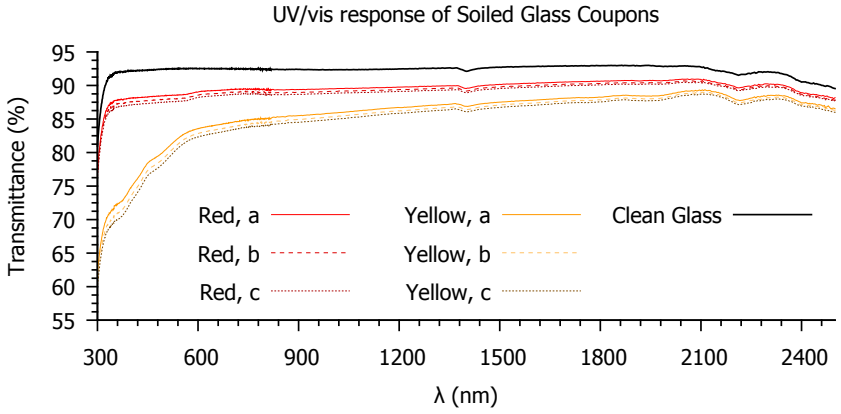

Figure C.2. DRA transmission measured through three coupons each of red and yellow test grime and a clean reference.

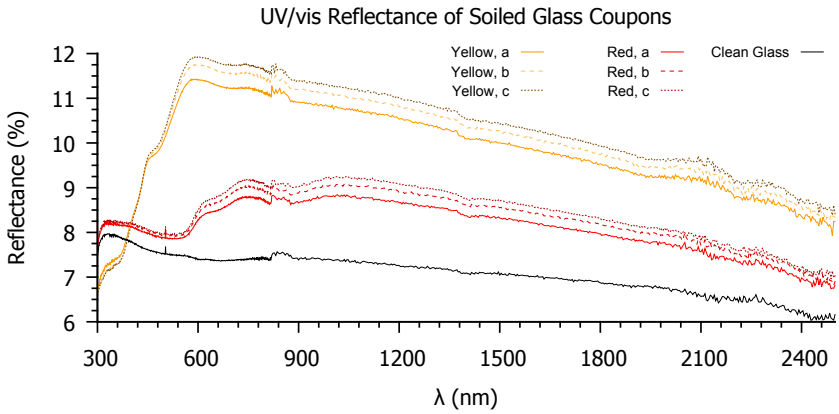

Figure C.3. Surface reflectance of red and yellow test grime and a clean reference.

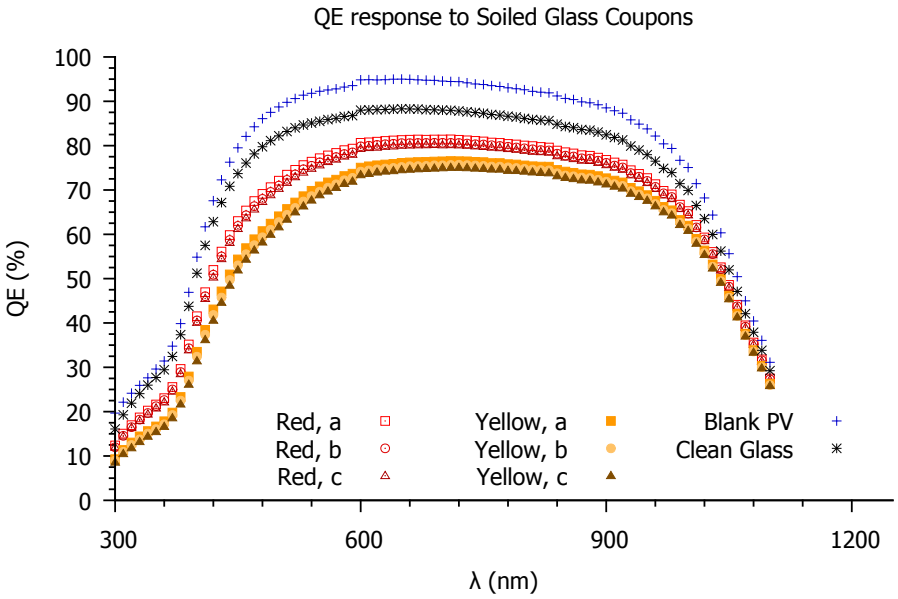

Figure C.4. Quantum efficiency measurements of red and yellow test grime and a clean reference.

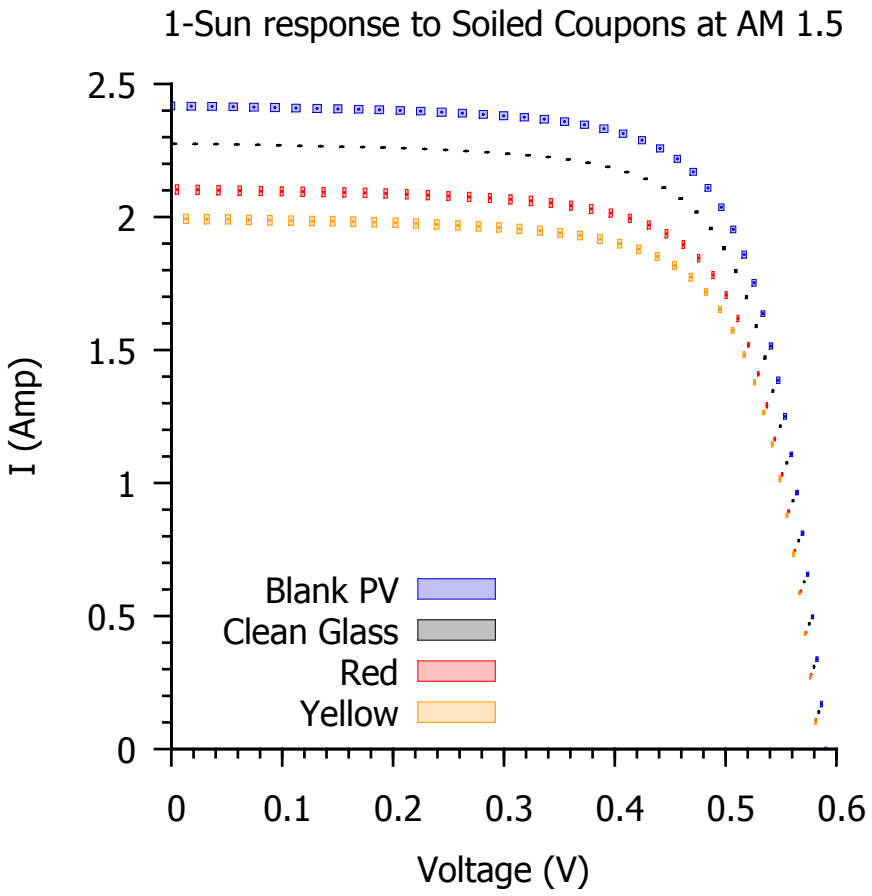

Figure C.5. One sun simulator measurements of red and yellow test grime and a clean reference.

DISTRIBUTION:

1	MS 0734	Patrick D. Burton, 6632
1	MS 0734	J. Bruce Kelly, 6632
1	MS 0951	Bruce H. King, 6112
1	MS 1033	Abe Ellis, 6112
1	MS 1104	Charles Hanley, 6110
1	MS 0899	Technical Library, 9536 (electronic copy)

Sandia National Laboratories